Vacuum-UV (172 nm) Actinometry. The Quantum Yield of the Photolysis of Water

Gernot Heit, Annette Neuner, Pierre-Yves Saugy, and André M. Braun*

Lehrstuhl für Umweltmesstechnik, Engler-Bunte-Institut, Universität Karlsruhe (TH), D-76128 Karlsruhe, Germany

Received: November 7, 1997; In Final Form: April 6, 1998

With the development of new light sources (Xe-excimer light sources), the vacuum-UV (VUV) photochemistry on a preparative scale is becoming technically feasible. Among the first potential technical applications, VUV photolysis of aqueous systems must be considered as a potential alternative to established "advanced oxidation procedures" (AOP). For the design and dimensioning of corresponding reactors, incident photon rates must be determined. The standard VUV actinometry in condensed phase is the cis−trans isomerization of cyclooctene in *n*-pentane. The incident photon rate of these new light sources depends on their geometry, the configuration of their electrodes, and the dielectric constant of the solvent in the case where the substrate solution is part of the dielectric barrier; thus actinometric experiments should be made under operational conditions. However, the radiant power density of the excimer sources will be different if *n*-pentane (standard actinometry) is used as part of the dielectric barrier from when using water (oxidative degradation experiments), because the voltage drop across the fluids is different. Consequently, for projects involving aqueous reactions systems, operational conditions cannot be met by the standard actinometer. Water exhibits a high absorption cross-section for VUV irradiation ($\lambda < 190$ nm) and homolyzes mainly into hydroxyl radicals and hydrogen atoms. Hydroxyl radicals, but not hydrogen atoms, are very efficiently scavenged by methanol molecules, and under defined conditions, the rate of production of hydroxyl radicals may be determined from the rate of degradation of methanol dissolved in the aqueous reaction system. The parameters affecting primarily the rate of methanol degradation, i.e., the incident photon rate, the concentration of dissolved molecular oxygen, the initial methanol concentration, and the flow parameters in the photochemical reactor, were determined and optimized for a general actinometric procedure. A normalized diagram of the incident photon rate versus the initial methanol concentration allows one to determine the boundary conditions under which the rate of methanol degradation may be used to evaluate the production rate of hydroxyl radicals for Xe-excimer light sources of different radiant power and independent of their geometry. Having determined both the rate of production of hydroxyl radicals and the rate of methanol degradation, and having calibrated the corresponding incident photon rates by the cis−trans isomerization of cyclooctene (standard actinometry) in an experimental setup in which the emitted photon rate does not depend on the reaction medium, the quantum yield of the homolysis of water by VUV irradiation from Xe-excimer lamps may finally be calculated.

Introduction

Xe-Excimer Light Sources.[1,2] The Xe-excimer light source is a so-called high-pressure dielectric barrier discharge (silent discharge) lamp. Collisions of high-energetic electrons (ca. 10 eV) with Xe atoms in the ground state lead to exited Xe atoms (reaction 1).

$$Xe + e^- \rightarrow Xe^* + e^- \quad (1)$$

$$Xe^* + 2Xe \rightarrow Xe_2^* + Xe \quad (2)$$

$$Xe_2^* \rightarrow 2Xe + h\nu \quad (3)$$

In subsequent collisions of two Xe atoms in their ground state with one exited Xe atom, a Xe-excimer (Xe_2^*) is created (reaction 2). Deactivation of the Xe-excimer leads to two Xe atoms in the ground state and produces a photon in the VUV spectral region. The emission spectrum of this light source shows a relatively narrow band with an emission maximum at 172 nm and a half-width of less than 14 nm (Figure 1).[3]

Free electrons are accelerated in an alternating electric field (ca. 10 kV, 150 kHz, depending on gap distance and gas pressure) between two electrodes to reach the energy required for exciting Xe atoms (reaction 1). Because of the presence of a dielectric barrier (Figure 2b,c), a gas discharge is quickly terminated and prevented from degenerating into a thermal arc. As long as these light sources are not ignited, they may be characterized as a serial arrangement of capacitors.[3] In practice, the light sources are constructed in a way that the space in which the light-emitting process takes place is enclosed by a VUV-transparent dielectric (e.g., synthetic quartz) with both electrodes shielded by these barriers (Figure 2b).

To minimize radiation losses (e.g., by additional quartz tubes or metal nets as outer electrodes), the design of photochemical reactors permits in many cases a direct contact of the substrate solution and the outer wall of the light source (Figure 2c). But under such experimental conditions, a strong dependence of the emitted photon rate from the reaction medium is observed.[4]

Reaction Manifold of VUV-Irradiated Water.[4−12] Water exhibits a high absorption cross-section for VUV radiation and homolyzes upon excitation into the primary radicals, hydrogen

* Author to whom correspondence should be addressed.

S1089-5639(98)00130-3 CCC: $15.00
Published on Web 05/27/1998

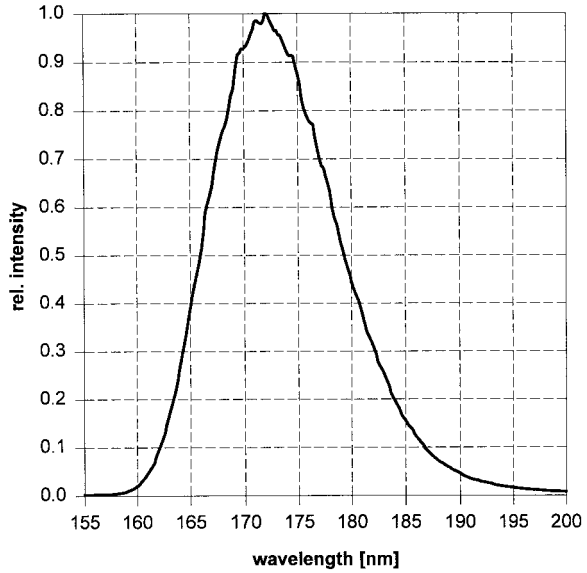

Figure 1. Emission spectrum of a Xe-excimer light source.[3]

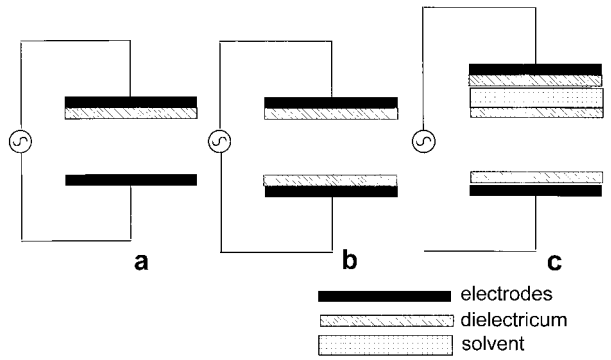

Figure 2. Schematic mountings of excimer light sources.

atoms, and hydroxyl radicals (reaction 4). Hydrated electrons are produced (reaction 5) on a smaller scale.

$$H_2O \xrightarrow{h\nu} HO^\bullet + H^\bullet \quad (4)$$

$$H_2O \xrightarrow{h\nu} HO^\bullet + H^+ + e^- \quad (5)$$

The linear absorption coefficient of pure water (k_{H_2O}) at the wavelength of the peak emission of the Xe-excimer light sources (172 nm) is ca. 550 cm^{-1}.[13]

The subsequent reactions of these primary radicals yield hydroperoxyl radicals, superoxide and oxide radical anions, hydroxide and hydroperoxide anions, and protons, leading finally to molecular oxygen, hydrogen peroxide, molecular hydrogen, and water.[4−12]

Reaction System of VUV-Irradiated Methanol. Methanol exhibits a very high absorption cross section in the VUV spectral region, the linear absorption coefficient (k_{MeOH}) at 172 nm being, at 4000 cm^{-1}, nearly 8 times higher than that of water.[13] Products and the quantum yield of the photochemical homolysis of methanol are only known for an excitation at 185 nm[14] and have been assumed to be unchanged for an excitation at 172 nm. At these wavelengths, methanol mainly homolyzes into methoxyl- and hydroxymethyl radicals, but also produces methyl radicals and formaldehyde (reactions 6−9).

$$CH_3OH \xrightarrow{h\nu} CH_3O^\bullet + H^\bullet \qquad \Phi = 0.69 \quad (6)$$

$$CH_3OH \xrightarrow{h\nu} HOCH_2^\bullet + H^\bullet \qquad \Phi = 0.08 \quad (7)$$

$$CH_3OH \xrightarrow{h\nu} CH_2O + H_2 \qquad \Phi = 0.06 \quad (8)$$

$$CH_3OH \xrightarrow{h\nu} CH_3^\bullet + HO^\bullet \qquad \Phi = 0.05 \quad (9)$$

Addition of these quantum yields leaves a quantum efficiency of ca. 12% for physical deactivation processes.

Reaction System of VUV-Irradiated Methanol in Aqueous Solutions.[7,8,14−18] Although the absorption cross section of pure methanol is much higher than that of water, at a ratio of $[MeOH]_0/[H_2O] \leq 2 \times 10^{-3}$ ($[H_2O] = 55$ mol L^{-1}) one may assume that photons are almost quantitatively absorbed by water molecules, leading to water homolysis.

For higher concentrations of methanol ($>10^{-1}$ mol L^{-1}), the linear absorption coefficient of the solution k at 172 nm has to be calculated:

$$k = k_{H_2O} + \epsilon_{MeOH}[MeOH] \quad (10)$$

with k_{H_2O} being the linear absorption coefficient of H_2O [cm^{-1}], $\epsilon_{MeOH} = k_{MeOH}/[MeOH]_{pure}$, and $[MeOH]_{pure} = 24.69$ mol L^{-1}.

In addition to the photochemical homolysis of methanol (reactions 6−9), degradation of methanol is initiated by reactions 11 and 12, yielding hydroxymethyl radicals.

$$CH_3OH + HO^\bullet \rightarrow HOCH_2^\bullet + H_2O \qquad k = 9.7 \times 10^8 \text{ L mol}^{-1} \text{ s}^{-1} \quad (11)$$

$$CH_3OH + H^\bullet \rightarrow HOCH_2^\bullet + H_2 \qquad k = 2.6 \times 10^6 \text{ L mol}^{-1} \text{ s}^{-1} \quad (12)$$

In the presence of molecular oxygen, these radicals are immediately oxidized to the corresponding peroxyl radicals.

$$HOCH_2^\bullet + O_2 \rightarrow {}^\bullet OOCH_2OH \qquad k = 4.9 \times 10^9 \text{ L mol}^{-1} \text{ s}^{-1} \quad (13)$$

In oxygen free solutions, hydroxymethyl radicals may disproportionate to methanol and formaldehyde (reaction 14) or recombine to ethylene glycol (reaction 15).

$$2HOCH_2^\bullet \rightarrow CH_3OH + CH_2O \qquad k = 2.0 \times 10^8 \text{ L mol}^{-1} \text{ s}^{-1} \quad (14)$$

$$2HOCH_2^\bullet \rightarrow (CH_2OH)_2 \qquad k = 1.0 \times 10^9 \text{ L mol}^{-1} \text{ s}^{-1} \quad (15)$$

The rate constant of reaction 15 being 5 times higher than that of reaction 14, 17% of the consumed methanol molecules (reactions 11 and 12), at the most (absence of oxygen), will be led back to methanol (reaction 14). The rates of production of ethylene glycol (reaction 15) and formaldehyde (reaction 14) may be determined experimentally, and consequently, the rate of hydroxymethyl radicals reacting to methanol (reaction 14) may be calculated.

In the presence of molecular oxygen, the sequence of reactions toward mineralization continues by reaction 16, leading to formate ions.

$$2{}^\bullet OOCH_2OH \rightarrow 2HCOO^- + 2H^+ + H_2O_2 \qquad k = 2.1 \times 10^9 \text{ L mol}^{-1} \text{ s}^{-1} \quad (16)$$

Formate ion and formic acid react with hydrogen atoms or hydroxyl radicals to form the protonated or deprotonated formyl radical:

$$H^{\bullet} + HCOOH \rightarrow H_2 + HCOO^{\bullet} \qquad k = 6.1 \times 10^7 \text{ L mol}^{-1} \text{ s}^{-1} \quad (17)$$

$$H^{\bullet} + HCOO^- \rightarrow H_2 + {}^{\bullet}COO^- \qquad k = 2.1 \times 10^8 \text{ L mol}^{-1} \text{ s}^{-1} \quad (18)$$

$$HO^{\bullet} + HCOOH \rightarrow H_2O + HCOO^{\bullet} \qquad k = 1.3 \times 10^8 \text{ L mol}^{-1} \text{ s}^{-1} \quad (19)$$

$$HO^{\bullet} + HCOO^- \rightarrow H_2O + {}^{\bullet}COO^- \qquad k = 3.2 \times 10^9 \text{ L mol}^{-1} \text{ s}^{-1} \quad (20)$$

The reactions of the protonated and the deprotonated formyl radicals with molecular oxygen will finally lead to carbon dioxide:

$${}^{\bullet}COO^- + O_2 \rightarrow CO_2 + O_2^{\bullet -} \qquad k = 2.4 \times 10^9 \text{ L mol}^{-1} \text{ s}^{-1} \quad (21)$$

$$HCOO^{\bullet} + O_2 \rightarrow CO_2 + HO_2^{\bullet} \qquad k = 3 \times 10^9 \text{ L mol}^{-1} \text{ s}^{-1} \quad (22)$$

Formaldehyde and ethylene glycol react both with hydrogen atoms and hydroxyl radicals by way of H-abstraction:

$$CH_2O + HO^{\bullet} \rightarrow {}^{\bullet}CHO + H_2O \qquad k = 1 \times 10^9 \text{ L mol}^{-1} \text{ s}^{-1} \quad (23)$$

$$CH_2O + H^{\bullet} \rightarrow {}^{\bullet}CHO + H_2 \qquad k = 1 \times 10^7 \text{ L mol}^{-1} \text{ s}^{-1} \quad (24)$$

$$(CH_2OH)_2 + HO^{\bullet} \rightarrow {}^{\bullet}CHOHCH_2OH + H_2O \qquad k = 1.8 \times 10^9 \text{ L mol}^{-1} \text{ s}^{-1} \quad (25)$$

$$(CH_2OH)_2 + H^{\bullet} \rightarrow {}^{\bullet}CHOHCH_2OH + H_2 \qquad k = 1.5 \times 10^7 \text{ L mol}^{-1} \text{ s}^{-1} \quad (26)$$

In the case of high incident photon density and, hence, of a high local density of hydroxymethyl radicals, oligomerization reactions with the radicals produced in reactions 25 and 26 lead to glycerin.

VUV Standard Actinometer in Condensed Phase: The Cis−Trans Isomerization of Cyclooctene in *n*-Pentane. The cis−trans isomerization of cyclooctene used as an actinometer for the determination of incident photon rates of low-pressure mercury lamps at 185 nm[19−21] has been modified to determine the incident photon rates of Xe-excimer lamps at 172 nm.[22]

Upon irradiation at 172 nm of an alkane solution (e.g., *n*-pentane) of commercially available *cis*-cyclooctene under oxygen-free conditions a photostationary state of *cis*- and *trans*-cyclooctene is reached.

In contrast to the earlier investigations where the kinetics of this reaction system has been solved, assuming that no photochemical degradation of cyclooctene would take place, we propose in this work to restrict analysis and calculations to the very beginning of the photochemical *cis*- to *trans*-isomerization, where a pure pseudo-first-order kinetics is found. To restrict the actinometry to this early period of the experiment means to provide a more sophisticated analytical procedure to determine the rates of *cis*-cyclooctene diminution and the *trans*-cyclooctene production with acceptable experimental errors. This modified actinometry also provides a technical advantage, as it may be carried out with commercially available *n*-pentane (p.a.), hence, simplifying considerably the experimental conditions.[4,23]

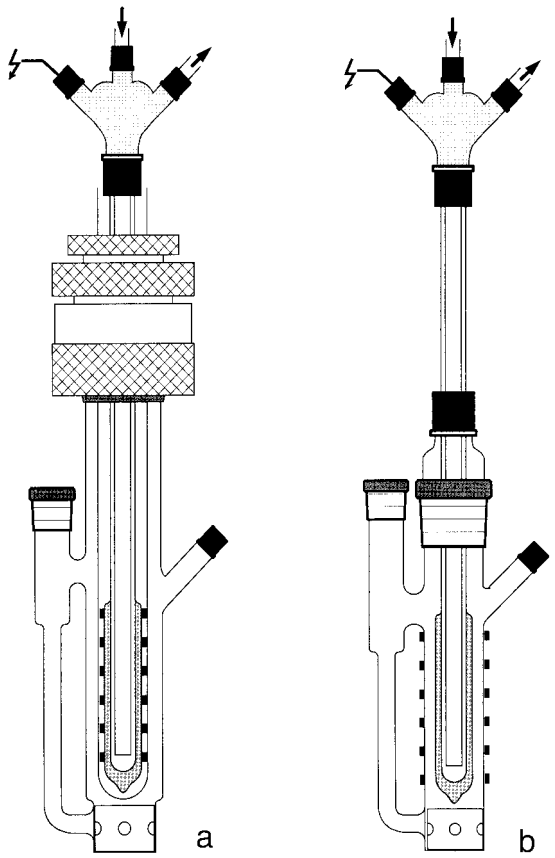

Figure 3. Experimental setup: batch system.

Experimental Part

Materials. Methanol (RotiSolv/HPLC, Roth), formaldehyde (37%, Aldrich ACS), formic acid (98%, p.a., Fluka), and ethylene glycol (p.a., Roth) were used without further purification. Solutions prepared with tridistilled water were saturated with synthetic air, nitrogen, or oxygen (Messer Griesheim). *n*-Pentane (p.a., Roth) as solvent for the cis−trans isomerization of cyclooctene was either used without further purification or purified by distillation under ambient pressure using an insulated packed column of 140 cm length and about 30 mm diameter.

Experiments. A number of 200 W (max.) Xe-excimer lamps were used for the photolysis of oxygen free (saturated with nitrogen), air-saturated, or oxygen-saturated aqueous solutions of methanol ($\leq$1 mol L^{-1}). The Xe-excimer lamps were build of two concentric Suprasil quartz tubes (outer diameters 30.4−26.2 mm; inner diameters 18.0−15.1 mm) and driven by a high-voltage power supply (ENI model HPG-2). The effective length of the light sources varied between 145 and 250 mm. The inner electrode (phase) consisted of an aluminum foil, cooled with distilled water.

The Xe-excimer lamps were used in two different experimental configurations. Experiments in batch mode were carried out in a loop-type photochemical reactor using two different configurations (Figure 3). In both reactors, the solutions were circulated by means of a PTFE-covered magnetic stirrer placed at the bottom of the reactor, the solution flowing down along

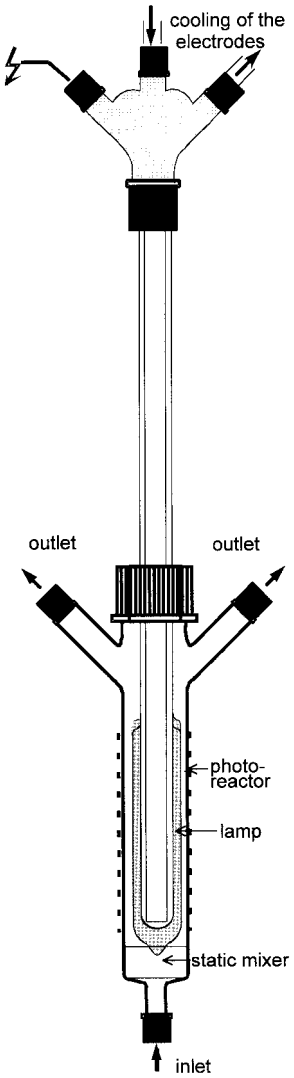

Figure 4. Experimental setup: semibatch system.

the lamp and up through the external bypass. The configuration represented in Figure 3b consisted of a smaller reactor with a total volume of 270 mL. The outer electrode was a metal net fixed around the outer wall of the reactor and connected to the ground. Alternatively, the irradiated solution was connected to the ground and served as outer electrode. In both cases, the irradiated reaction system is in direct contact with the surface of the light source. In the reactor configuration represented in Figure 3a, a larger reactor volume (350 mL) is used, and an additional synthetic quartz tube is positioned between the outer wall of the light source and the reaction solution, providing a gap for the outer electrode. Because the solution is located outside the grounded electrode, this configuration avoids any effect of the solvent and/or substrate parameters on the radiant efficiency of the light source. This outer electrode was cooled by nitrogen, avoiding filter effects by molecular oxygen. For all experiments, the reactors were immersed into a thermostated (25 °C) water bath to ensure constant process temperature.

In semibatch experiments, nitrogen-, air-, or oxygen-saturated aqueous methanol solutions were continuously circulated between an immersion-type photochemical reactor and a reservoir of 65 and 1000 mL volume, respectively, passing a static mixer (Figure 4). The solutions entered the reactor through the inlet at the bottom of the reactor, streamed up along the lamp, and left the reactor by the two outlets at the top toward the reservoir. Because of continuous gas saturation, the solutions entering the photoreactor were assumed to be nitrogen, air, or oxygen saturated. The reservoir was thermostated at 25 °C. A metal net fixed around the outer wall of the reactor and connected to the ground served as outer electrode. In a number of experiments, the irradiated solutions were connected to the ground, and no additional electrode was used.

Analysis. Purification of *n*-pentane was tested and the concentrations of cyclooctene were analyzed by GC analysis (Hewlett-Packard 5890 series II), as described elsewhere.[22,23] The degradation of methanol and the production of ethylene glycol were also followed by GC analysis (Hewlett-Packard 5890 series II, HP-Innowax column, length 30 m, inner diameter 0.32 mm, film thickness: 0.52 μm; pre-column, length 1 m, inner diameter 0.52 mm). Applying a temperature gradient, both components may be analyzed in one analysis: during the retention time of methanol (ca. 2 min), the oven temperature was kept constant at 115 °C, then quickly increased to 180 °C, and kept at this temperature until the end of the analysis (ca. 8 min). Finally, the column was rapidly heated up to 220 °C.

Formaldehyde concentrations were determined in producing the corresponding 2,4-dinitrophenylhydrazone, which was analyzed by HPLC analysis (HP chromatograph series 1050 with UV detector, RP18 column) at its absorption maximum at 360 nm.

Formic acid, oxalic acid, and glycolic acid were analyzed under isothermal conditions (35 °C) by IC using a conductometer as detector (Dionex, column AS12A, 200 × 4 mm with pre-column AG12A, 50 × 4 mm). The eluent consisted of a sodium carbonate/bicarbonate solution (2.7/0.3 mol L^{-1}); the flow rate was fixed at 1.5 mL min^{-1}.

The diminution of dissolved organic matter was measured by a DOC analyzer (Dohrmann DC-190).

Results and Discussion

Methanol Degradation in Aqueous VUV-Irradiated Solutions. Upon VUV irradiation (Xe-excimer light sources, 172 nm) of aqueous solutions of methanol, the organic substrate is oxidized and ethylene glycol, formic acid, glycolic acid, and formaldehyde were analyzed as intermediates of mineralization. Oxalic acid, however, was not observed. The results of the irradiation experiments are summarized in Figures 5, 6, and 7. They show the concentrations of methanol, ethylene glycol, formaldehyde, glycolic acid, and DOC as a function of irradiation time in oxygen-free (Figure 5), air-saturated (Figure 6), and oxygen-saturated solutions (Figure 7). For all these photolysis experiments reported, Xe-excimer lamps were used in a semibatch reactor (Figure 4), the electrical input power being set at 150 W.

Taking into account that the rate constant of reaction 11 is about 100 times higher than that of reaction 12 as well as the high efficiency of reaction 27, the reaction of methanol with hydrogen atoms (reaction 12) may be neglected.

$$H^{\bullet} + O_2 \rightarrow HO_2^{\bullet} \qquad k = 2 \times 10^{10}\ \mathrm{L\ mol^{-1}\ s^{-1}} \quad (27)$$

Confirming this hypothesis, the rate of methanol degradation did not increase with the diminution of the concentration of dissolved molecular oxygen. Diminution of methanol concentration being primarily caused by the reaction with hydroxyl radicals and, to a lesser extent, by VUV photolysis, the relation between the incident photon rate P_0, assuming total absorbance

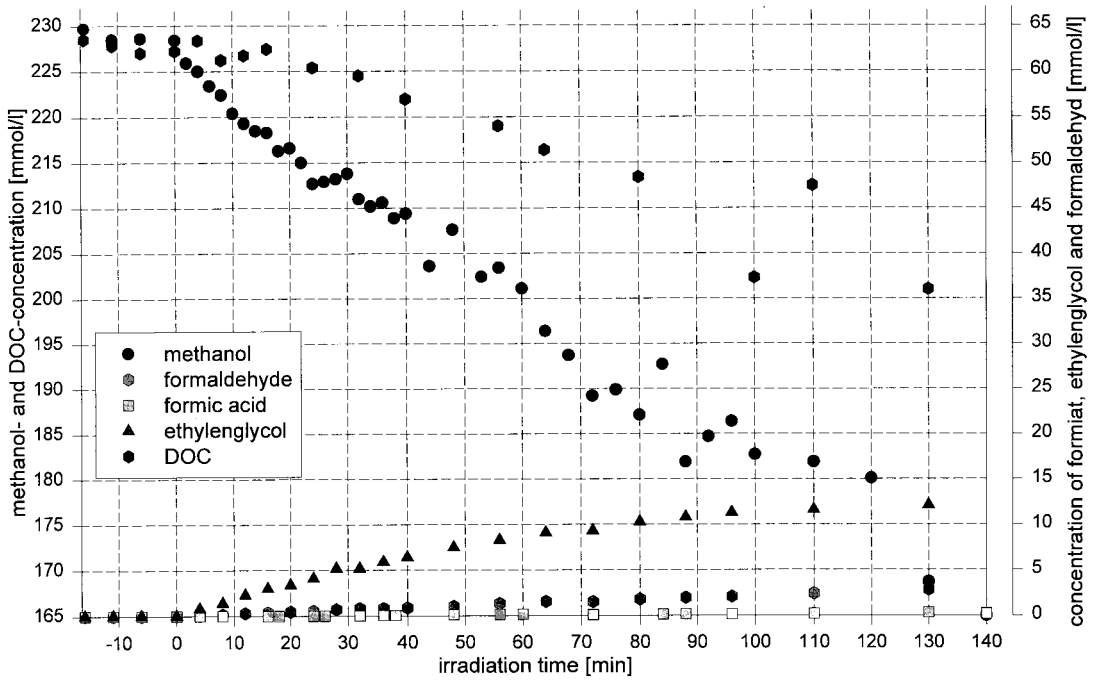

Figure 5. Methanol and product concentrations and DOC values as a function of irradiation time (VUV-irradiated aqueous solution of methanol in the absence of oxygen (continuous purging with nitrogen)).

($P_a = P_0$), and the rate of methanol degradation may be given as

$$\frac{\Phi P_0}{V_R} = \left.\frac{\mathrm{d[MeOH]}}{\mathrm{d}t}\right|_{\mathrm{OH},h\nu} = \frac{\mathrm{d[MeOH]}}{\mathrm{d}t} + \left.\frac{\mathrm{d[MeOH]}}{\mathrm{d}t}\right|_{14} \quad (28)$$

where P_a = the absorbed photon rate [einstein s^{-1}]; V_R = the total volume of the reactor [L]; Φ = the quantum yield of apparent methanol degradation with

$$\Phi = (\xi_{\mathrm{MeOH}}\Phi_{\mathrm{MeOH}} + \phi_R\xi_{\mathrm{H_2O}}\Phi_{\mathrm{H_2O}}) \quad (29)$$

ζ_i = the fraction of the photon rate absorbed by component i with

$$\zeta_i = k_i/\Sigma k_i \quad (30)$$

with k_i = linear absorption coefficient of the component i [cm^{-1}]; Φ_{MeOH} = the sum of quantum yields of reactions 6−9; ϕ_R = the efficiency of hydroxyl radical scavenging in reaction 11; $\Phi_{\mathrm{H_2O}}$ = the sum of quantum yields of reactions 4 and 5; $(\mathrm{d[MeOH]/d}t)|_{\mathrm{OH},h\nu}$ = the total rate of methanol photolysis (reactions 6−9 and 11) yielding hydroxymethyl radicals; $\mathrm{d[MeOH]/d}t$ = the apparent (measured) rate of methanol degradation; and $(\mathrm{d[MeOH]/d}t)|_{14}$ = the rate of methanol production by reaction 14.

Since $(\mathrm{d[MeOH]/d}t|_{14}$ may be evaluated experimentally, and the rate constants of reactions 31 and 34 are known,

$$\mathrm{HO^\bullet + HO^\bullet \rightarrow H_2O_2} \qquad k = 5.5 \times 10^9\ \mathrm{L\ mol^{-1}\ s^{-1}} \quad (31)$$

$$\mathrm{HO^\bullet + H_2O_2 \rightarrow HO_2^\bullet + H_2O} \qquad k = 2.7 \times 10^7\ \mathrm{L\ mol^{-1}\ s^{-1}} \quad (32)$$

$$\mathrm{HO^\bullet + HO_2^\bullet \rightarrow O_2 + H_2O} \qquad k = 6 \times 10^9\ \mathrm{L\ mol^{-1}\ s^{-1}} \quad (33)$$

$$\mathrm{HO^\bullet + H^\bullet \rightarrow H_2O} \qquad k = 7 \times 10^9\ \mathrm{L\ mol^{-1}\ s^{-1}} \quad (34)$$

the quantum yield of methanol degradation (reactions 28, 29) may be calculated, once the incident photon rate and $\mathrm{d[MeOH]/d}t$ have been determined experimentally. The quantum efficiency of water homolysis may then be calculated from the quantum yield of methanol degradation and the absorption cross sections of methanol and water at the wavelength of irradiation (eqs 29 and 30). All these data finally permit one to establish a procedure to determine the incident photon rate in measuring the rate of degradation of methanol.

Intermediate formation of ethylene glycol and formaldehyde depends on the concentration of dissolved molecular oxygen (eqs 13−15). The ratio of the rate of methanol degradation to that of ethylene glycol production increases from 2.9 in oxygen-free solutions to 4.4 in air-saturated and to 6.5 in oxygen-saturated solutions. The discrepancy between this experimentally determined value in oxygen free solutions and the ratio evaluated in taking the published reaction rate constants of reactions 14 and 15 is most probably due to oxygen production in VUV-irradiated aqueous systems (vide supra) and its immediate impact on the reaction manifold in initially oxygen-free reaction systems. Consequently, even in oxygen free solutions a fraction of hydroxymethyl radicals from reactions 11 and 12 reacts to hydroxymethylperoxyl radicals (eq 13), and the experimentally determined ratio between the degradation rate of methanol to the production rate of ethylene glycol will always be higher than the calculated ratio.

By analogy, the ratio of the rate of degradation of methanol to the production rate of formaldehyde increases from oxygen-free solutions with a value of 14.9 to air-saturated solutions, where a ratio of 17.8 has been determined.

As expected from the published rate constants of reactions 14 and 15, the rate of ethylene glycol production is about 5 times higher than the production rate of formaldehyde (experimentally determined ratio: 5.1) in oxygen-free solutions. In air-saturated solutions, this ratio is reduced to 4.4 most probably due to reaction 35.

$$\mathrm{^\bullet OOCH_2OH \rightarrow CH_2O + O_2^{\bullet -} + H^+} \qquad k = 10\ \mathrm{s^{-1}} \quad (35)$$

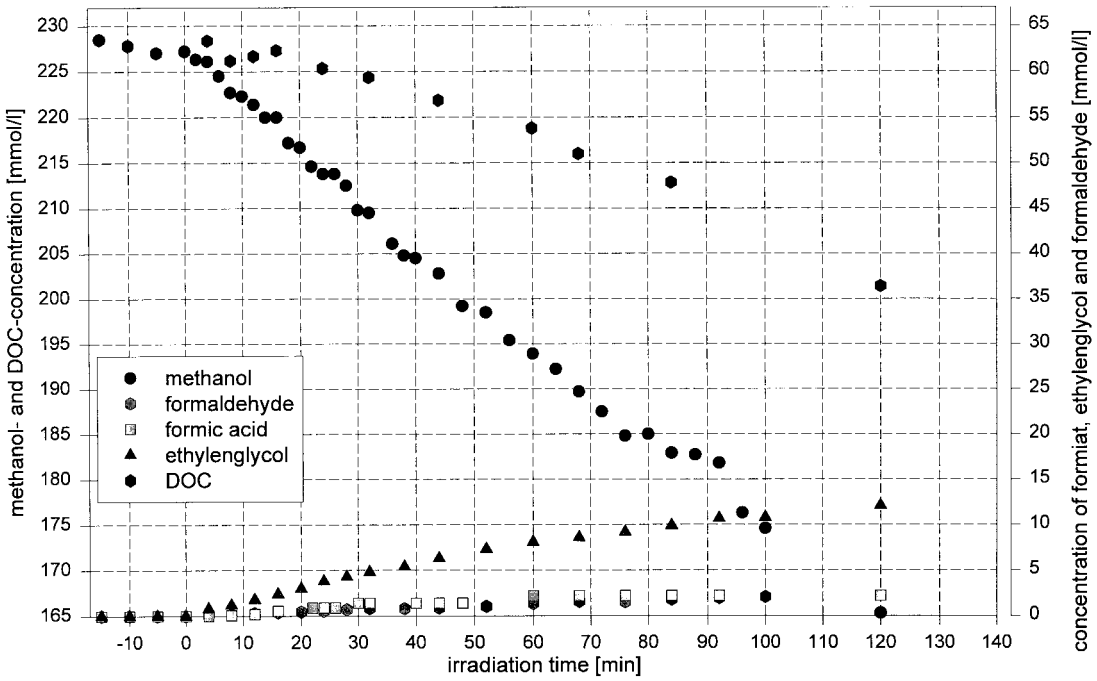

Figure 6. Methanol and product concentrations and DOC values as a function of irradiation time (VUV-irradiated aqueous solution of methanol).

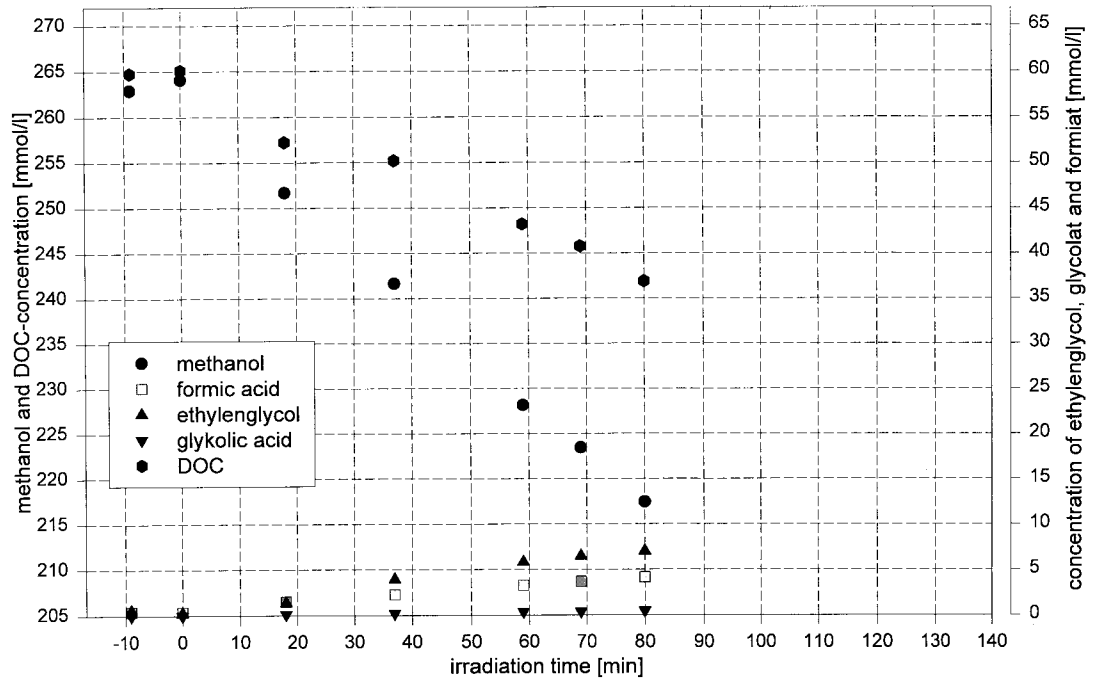

Figure 7. Methanol and product concentrations and DOC values as a function of irradiation time (VUV-irradiated aqueous solution of methanol (continuous purging with oxygen)).

Knowing the interdependence of the rate of methanol degradation and the rates of ethylene glycol (EG) and formaldehyde production, respectively, the rate of methanol production by disproportionation (eq 14) may be calculated for oxygen-free solutions by

$$\left.\frac{\mathrm{d[MeOH]}}{\mathrm{d}t}\right|_{14} = 0.2\frac{\mathrm{d[EG]}}{\mathrm{d}t} \qquad (36)$$

In analyzing under these experimental conditions simultaneously ethylene glycol and methanol, the rate of methanol production by eq 14 may be calculated from the rate of ethylene glycol production using eq 36.

For experiments carried out in air-saturated solutions, the rate of ethylene glycol production was found to be 0.288 ± 0.015 times the rate of methanol degradation.[4] This value is higher than expected and is a consequence of the low local concentration of dissolved molecular oxygen in the irradiated reactor volume. In fact, it has been shown that the oxygen concentration varies locally in VUV-irradiated aqueous systems,[4,24,25] the very restricted irradiated reactor volume being rapidly depleted of oxygen.

Even though molecular oxygen is built up by reactions 31−33 in oxygen- and air-saturated solutions, too, oxygen-consuming reactions 27, 37, and 13 will be dominant and the oxygen concentration within the irradiated layer will be reduced.

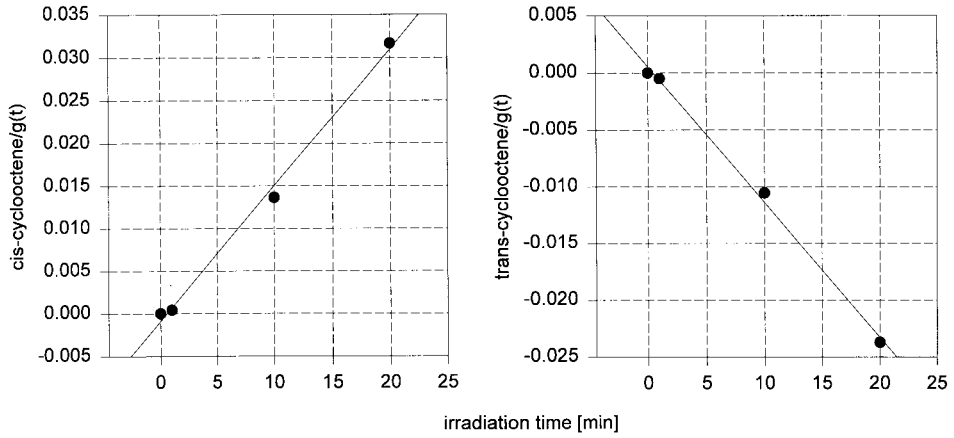

Figure 8. Ratios of *cis*- and *trans*-cyclooctene, respectively, over $g(t)$ as a function of irradiation time.

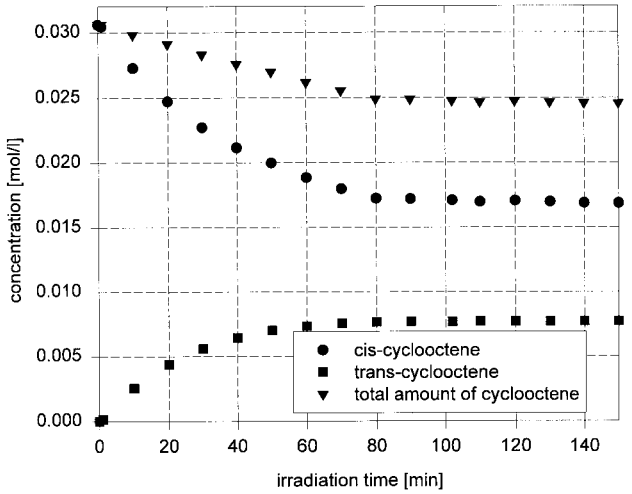

Figure 9. Concentrations of *cis*- and *trans*-cyclooctene and the total concentration of cyclooctenes as a function of irradiation time.

$$e^- + O_2 \rightarrow O_2^{\bullet -} \qquad k = 1 \times 10^{10}\ \mathrm{L\ mol^{-1}\ s^{-1}} \quad (37)$$

The production of ethylene glycol in oxygen-saturated solutions therefore indicates that the concentration of molecular oxygen in this irradiated layer is low enough that reaction 15 may compete with reaction 13, although the rate of reaction 15 depends on the squared value of a low intermediate concentration of the hydroxymethyl radicals and has the disadvantage of a lower rate constant.

In the case where reactions 6−9 are negligible (low methanol concentration), the rate of reaction 11 may be calculated by

$$\left.\frac{\mathrm{d[MeOH]}}{\mathrm{d}t}\right|_{\mathrm{OH}} = \frac{\mathrm{d[MeOH]}}{\mathrm{d}t} + \left.\frac{\mathrm{d[MeOH]}}{\mathrm{d}t}\right|_{14} = (1 + 0.2 \times 0.29)\frac{\mathrm{d[MeOH]}}{\mathrm{d}t} = 1.058\frac{\mathrm{d[MeOH]}}{\mathrm{d}t} \quad (38)$$

The manifold of reactions suggests that the rate of methanol consumption depends only in an insignificant way on the concentration of dissolved molecular oxygen. In fact, in air-saturated solutions, the rate of methanol degradation is lower by less than 6% in comparison to that in oxygen-saturated solution. The rate of the competing methanol production by disproportionation (eq 14) is lower by 50% in oxygen-saturated solution, but higher by less than 50% in oxygen-free solution compared to air-saturated solution. These data show that there is practically no effect on the overall rate of methanol degradation by changing the concentration of dissolved molecular oxygen, variations of experimentally determined values remaining within the limits of experimental error.

It should also be noted that the rate of methanol degradation does not depend on the flow characteristics within the limits of the equipment available ($700 < \mathrm{Re} < 2800$).

TABLE 1: Molecular Absorption Coefficients of Cyclooectene Isomers and Quantum Yields Φ of Cyclooctene Isomerization[3]

	ϵ [L mol^{-1} cm^{-1}]	Φ [mol einstein^{-1}]
cis-cyclooctene	6130	$\Phi_{cis} = 0.32$ (cis→trans)
trans-cyclooctene	7490	$\Phi_{trans} = 0.44$ (trans→cis)

Determination of the Quantum Yield of the Homolysis of Water upon Excitation at 172 nm. Using the batch equipment depicted in Figure 3a, effects of changes of the reaction systems on the performance of the light source are excluded. The reactor may therefore be used for determining the incident photon rate by means of the cis−trans isomerization of cyclooctene in *n*-pentane as well as the rate of methanol degradation in aqueous solutions. From these data, the quantum yield of methanol degradation Φ (eq 28) as well as the quantum yield of water homolysis (eq 29) may be calculated.

Molecular absorption coefficients of *cis*- and *trans*-cyclooctene and quantum yields Φ_{cis} and Φ_{trans} of the production of *trans*- and *cis*-cyclooctene, respectively, are shown in Table 1. The fractions of the photon rate absorbed by *cis*-cyclooctene, ζ_{cis}, and by *trans*-cyclooctene, ζ_{trans}, are independent of the penetration depth of the light. Adapting eq 30 to these conditions, we may write

$$\zeta_{cis} = \frac{\left.\frac{\mathrm{d}P_a}{\mathrm{d}x}\right|_{cis}}{\left.\frac{\mathrm{d}P_a}{\mathrm{d}x}\right|_{total}} = \frac{\epsilon_{cis}c_{cis}}{\epsilon_{cis}c_{cis} + \epsilon_{trans}c_{trans}} \neq f(x) \quad (30a)$$

and

$$\zeta_{trans} = \frac{\left.\frac{\mathrm{d}P_a}{\mathrm{d}x}\right|_{trans}}{\left.\frac{\mathrm{d}P_a}{\mathrm{d}x}\right|_{total}} = \frac{\epsilon_{trans}c_{trans}}{\epsilon_{cis}c_{cis} + \epsilon_{trans}c_{trans}} \neq f(x) \quad (30b)$$

TABLE 2: Results of the Standard VUV (Cyclooctene) Actinometry. Incident Photon Rates of the Xe-Excimer Lamp (λ_{exc}: 172 nm) of 130 W Placed into the Reactor Shown in Figure 3a

[*cis*-cyclooctene]$_0$ [mol L^{-1}]	purity of pentane [%]	P_0 [einstein min^{-1}]	P_0 [W]
0.0306	>99.95	3.5×10^{-4}	
		4.2×10^{-4}	
0.0321	>99.98	3.6×10^{-4}	
		4.6×10^{-4}	
		$(4.0 \pm 0.51) \times 10^{-4}$	4.6 ± 0.6

The rates of cyclooctene isomerization may then be described by the differential equation

$$\frac{dc_{trans}(t)}{dt} = -\frac{dc_{cis}(t)}{dt} = \left|\frac{dc_i(t)}{dt}\right| = \{\Phi_{cis}\zeta_{cis}(t) - \Phi_{trans}\zeta_{trans}(t)\}\frac{P_a}{V_R} = g(t)\frac{P_a}{V_R} \quad (39)$$

with

$$g(t) = \Phi_{cis}\zeta_{cis}(t) - \Phi_{trans}\zeta_{trans}(t)$$

and may be solved assuming that

$$|c_i(t)| = |g(t)|t\frac{P_a}{V_R} \Leftrightarrow \left|\frac{c_i(t)}{g(t)}\right|V_R = tP_a \quad (40)$$

for

$$\left|\frac{\frac{\partial g(t)}{\partial t}t}{g(t)}\right| \ll 1 \quad (41)$$

For short irradiation times t (t < 20 min), condition 41 is satisfied, and by a linear fit of $|c_i(t)/g(t)|V_R = f(t)$ (Figure 8), the absorbed photon rate P_a can be determined.

For initial cyclooctene concentrations of 3.06×10^{-2} and 3.21×10^{-2} mol L^{-1} in purified (>99.98%) and unpurified *n*-pentane (>99.95%), respectively, the incident photon rate was determined to be $(4.0 \pm 0.51) \times 10^{-4}$ einstein min^{-1} or 4.6 ($\pm$ 0.6) W (Table 2) for an electrical input power of 130 W. The chosen cyclooctene concentrations ensure total absorption of the incident photon rate, i.e., $P_a = P_0$. The decay of *cis*- and the increase of *trans*-cyclooctene with irradiation time reaching a photostationary state is shown in Figure 9.

The rate of methanol degradation was measured using the same photochemical reactor of a total volume of 350 mL. Initial concentrations of methanol (0.299 and 0.208 mol L^{-1}) ensured $\phi_R = 1$. The electrical input power of the power supply was kept the same as for the actinometric experiments. The high absorption cross section of water guarantees total absorption of the incident photon rate within the optical path length of the chosen reactor. Additional data needed for the calculation of the quantum yield of water homolysis Φ_{H_2O} and the results are shown in Table 3. Together with the already reported values of Φ_{H_2O} for λ_{exc} = 185, 147, and 123 nm, respectively,[18] the resulting quantum yield for λ_{exc} = 172 nm fits well into the dependence of $\Phi_{H_2O} = f(\lambda_{exc})$ (Figure 10).[4]

TABLE 3: Quantum Yield Φ_{H_2O} of Water Homolysis at λ_{exc} = 172 nm

[MeOH]$_0$ [mol L^{-1}]	d[MeOH]/d$t|_{OH}V_R$ [mol min^{-1}]	Φ	Φ_{H_2O}
0.299	$0.17(3) \times 10^{-3}$	0.42(7)	0.38(7)
0.208	$0.18(7) \times 10^{-3}$	0.46(7)	0.44(3)
			$0.41(7) \pm 0.03$

Determination of the Rate of Hydroxyl Radial Production and the Initial Photon Rate of Xe-Excimer Light Sources Irradiating Aqueous Solutions. The initial rate of methanol degradation (conversion rate <15%) has been found to be constant for all experiments. The rate of hydroxyl radical production may be evaluated from the rate of methanol degradation in modifying eqs 28 and 29:

$$\left.\frac{d[MeOH]}{dt}\right|_{OH,h\nu} = \left.\frac{d[MeOH]}{dt}\right|_{OH} + \left.\frac{d[MeOH]}{dt}\right|_{h\nu} \quad (42)$$

$$\frac{d[HO^\bullet]}{dt} = \left.\frac{d[MeOH]}{dt}\right|_{OH} = \zeta_{H_2O}\phi_R\left.\frac{d[MeOH]}{dt}\right|_{OH,h\nu} = \zeta_{H_2O}\phi_R\frac{\Phi_{H_2O}P_0}{V_R} \quad (43)$$

Knowing Φ_{H_2O} and assuming experimental conditions, where all hydroxyl radicals react with methanol molecules ($\phi_R = 1$), the incident photon rate may be calculated for air saturated solutions in applying eqs 28 and 38:

$$P_0 = P_{0,app} = \left.\frac{d[MeOH]}{dt}\right|_{OH}\frac{V_R}{\Phi_{H_2O}\zeta_{H_2O}} = \left.\frac{d[MeOH]}{dt}\right|_{OH,h\nu}\frac{V_R}{\Phi} = \left.\frac{d[MeOH]}{dt}\right|_{OH,h\nu}\frac{V_R}{\Phi_{H_2O}\zeta_{H_2O} + \Phi_{MeOH}\zeta_{MeOH}} \quad (44)$$

$$= 1.0575\frac{d[MeOH]}{dt}\frac{V_R}{\Phi_{H_2O}\zeta_{H_2O} + \Phi_{MeOH}\zeta_{MeOH}}$$

In the domain of methanol concentrations for which ϕ_R < 1, increasing initial methanol concentration leads to faster methanol degradation until a limiting value is reached (Figure 11). At concentrations of methanol above this limit, recombination and back reaction of the hydroxyl radicals (eqs 31, 34) have not been taken into account, and reactions of organic intermediates with hydroxyl radicals may also be neglected within the time limit imposed. Under such conditions, the efficiency of eq 11 reaches 100% ($\phi_R = 1$).

The high absorption cross section of water, the high quantum efficiency of hydroxyl radical production, and the short lifetime of the hydroxyl radicals lead to a strong heterogeneity in the macroscopically homogenous reaction system.[4,24,25] We differentiate a volume of primary reaction close to the surface of the lamp, in which the rates of reactions 11 and 13 are controlled by the diffusion of the organic substrate and of molecular oxygen

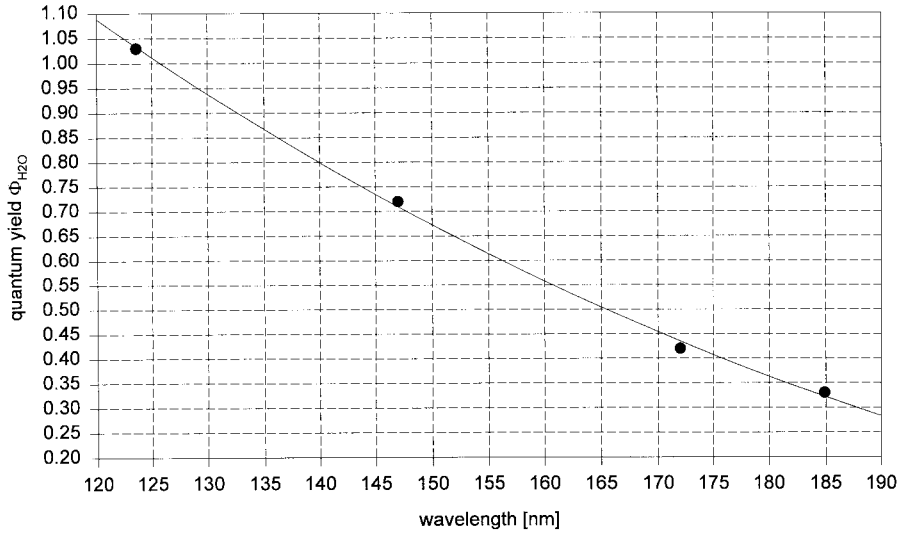

Figure 10. Quantum yield of water homolysis as a function of λ_{exc}.

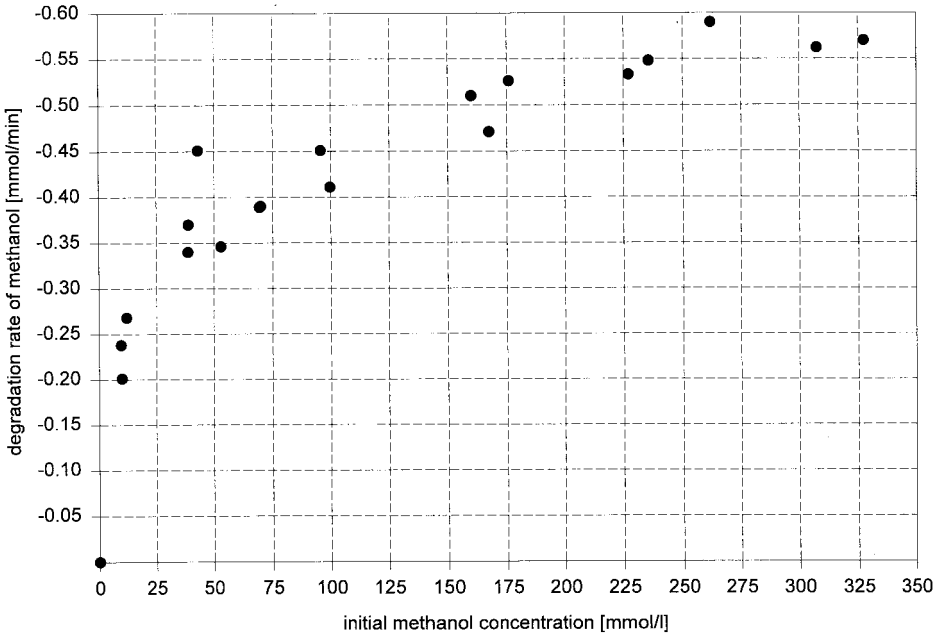

Figure 11. Rate of methanol degradation (10^{-3} mol min^{-1}) as a function of the initial methanol concentration (10^{-3} mol L^{-1}).

into this layer, and a large volume of secondary reactions, in which slower thermal reactions dominate.[4] To avoid the undesired reactions 31 and 34, not the macroscopic but the local concentration of methanol in the proximity of the surface of the light source is important. This local concentration may be estimated under photostationary conditions from the macroscopic concentration of methanol $[MeOH]_0$, the sum of absorption coefficients, and the diffusion coefficient of methanol in water D_{MeOH}. Assuming that hydroxyl radicals react quantitatively with methanol ($\phi_R = 1$) at the site of hydroxyl radical production, the local concentration of methanol close to the surface of the lamp, $[MeOH]_{surf}$, may be calculated in using eq 45.

$$[MeOH]_{surf} = \frac{(\zeta_{MeOH}\Phi_{MeOH} + \zeta_{H_2O}\Phi_{H_2O})P_0}{D_{MeOH}\sum k_i \ln(10)} + [MeOH]_0 \quad (45)$$

The minimum average concentration of methanol in the reaction system, $[MeOH]_{min}$, which ensures that the concentration of methanol on the surface of the lamp is above 0, is given by

$$[MeOH]_{min} = \frac{(\zeta_{MeOH}\Phi_{MeOH} + \zeta_{H_2O}\Phi_{H_2O})P_0}{D_{MeOH}\sum k_i \ln(10)} \quad (46)$$

The excess factor

$$n = \frac{[MeOH]_0}{[MeOH]_{min}} \quad (47)$$

describes how much the initial macroscopic concentration of methanol exceeds the minimum average concentration defined above. As the degradation rate of methanol only depends on the diffusion at and to the surface of the lamp, which may not be accelerated by flow phenomena, this excess factor n may be used as abscissa in a normalized diagram (Figure 12), which is valid independently of the Xe-excimer lamp used. To complete the normalization, the ordinate of Figure 12 represents the ratio between the apparent radiant power P_{app} in using eq 44 and the radiant power P_0 determined by actinometry. Expressed in a different way, this diagram shows the fraction of hydroxyl radicals that react with methanol as a function of the excess factor n as defined above.

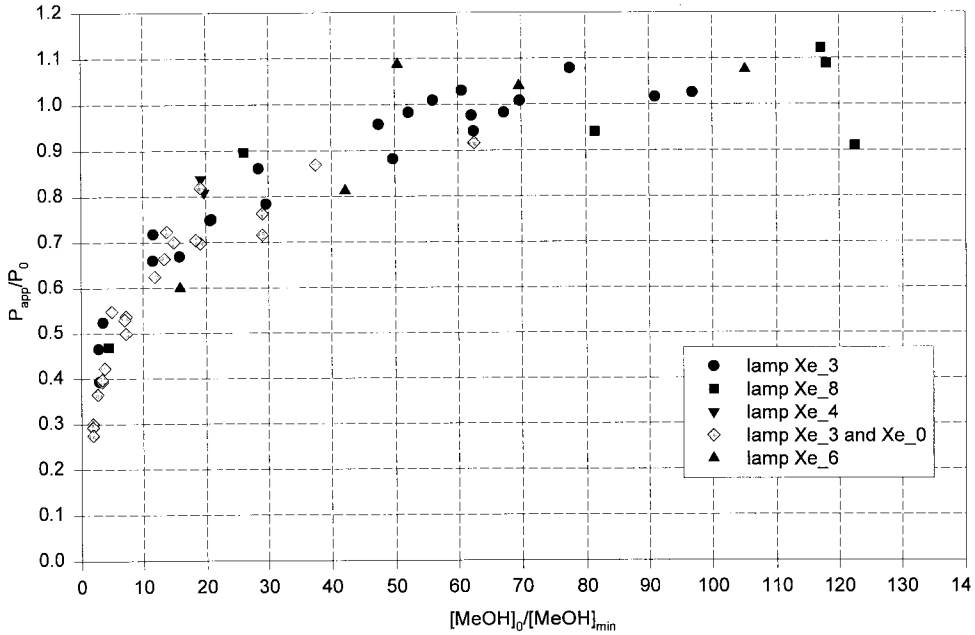

Figure 12. Normalized diagram of the measured (apparent) incident photon rate (einstein min^{-1}) as a function of the excess factor $n = [MeOH]_0/[MEOH]_{min}$.

For an excess factor $n > 70$, the calculated apparent radiant power P_{app} equals the effective radiant power of the lamp P_0. Above this value n, conditions for actinometry are accomplished.

The incident photon rate $P_0 = P_{app}$ may then be evaluated from the rate of methanol degradation using eq 44.

Conclusions

Measurements of the rate of methanol degradation represent an appropriate method for the determination of the rate of hydroxyl radical production in VUV-irradiated aqueous systems. As the limits and boundary conditions for the validity of this method are investigated and fixed in this work, the rate of hydroxyl radical production may easily be estimated by means of in situ measurements of the methanol concentration as a function of the time of irradiation. Care has to be taken that the actinometric measurements are made in the photochemical reactor that is used in the photochemical project.

Taking the rate of hydroxyl radical production calculated from the rate of methanol degradation and the absorbed photon rate which in turn has been determined by the standard VUV actinometry (cis−trans isomerization of cyclooctene in *n*-pentane), the quantum yield of hydroxyl radical production by Xe-excimer light sources, Φ_{H_2O}, could be determined to be 0.42 ± 0.04.

Based on this value, methanol degradation in VUV-irradiated aqueous solutions represents a new suitable actinometry for the in situ determination of incident photon rates of Xe-excimer light sources. This method is of importance in cases where Xe-excimer light sources are used for irradiating aqueous systems and their performance depending on the solvent properties.

The experimental error of these actinometric measurements is about 10%, including the fluctuations of the emission of the light sources due to temperature effects and variations within the electric and electronic equipment.

List of Symbols

c_i		concentration of cyclooctene isomers (mol L^{-1})
c_{cis}		concentration of *cis*-cyclooctene (mol L^{-1})
c_{trans}		concentration of *trans*-cyclooctene (mol L^{-1})
D_{MeOH}		diffusion coefficient of methanol in water
ϵ		molar extinction coeffcients [L mol^{-1} cm^{-1}]
at 172 nm	ϵ_{MeOH}	molar extinction coeffcient of CH_3OH (162 L mol^{-1} cm^{-1})
	ϵ_{cis}	molar extinction coeffcient of *cis*-cyclooctene (6130 L mol^{-1} cm^{-1})
	ϵ_{trans}	molar extinction coeffcient of *trans*-cyclooctene (7490 L mol^{-1} cm^{-1})
k		reaction rate constants
k_i		linear absorption coefficient of the component i [cm^{-1}]
at 172 nm	k	sum of linear absorption coefficients [cm^{-1}]
	k_{H_2O}	linear absorption coefficient of H_2O (550 cm^{-1})
	k_{MeOH}	linear absorption coefficient of CH_3OH (4000 cm^{-1})
$[MeOH]_0$		initial macroscopic (total) concentration of methanol (mol L^{-1})
$[MeOH]_{min}$		minimum average concentration of methanol in the reaction system which ensures that the concentration of methanol on the surface of the lamp is above 0 (mol L^{-1})
$[MeOH]_{surf}$		concentration of CH_3OH close to the surface of the light source (mol L^{-1})
n		excess factor (eq 47)
P_a		absorbed photon rates [einstein s^{-1}]
P_0		incident photon rates [einstein s^{-1}]
$P_{0,app}$		apparent incident photon rates [einstein s^{-1}] or apparent radiant power [W]
Φ		quantum yields
at 172 nm	Φ	quantum yield of apparent methanol degradation
	Φ_{MeOH}	quantum yield of CH_3OH photolysis (reactions 6−9)
	Φ_{H_2O}	quantum yield of H_2O photolysis (reactions 4 and 5)
ϕ_R		efficiency of reaction 11

pK_a		negative logarithmic values of acid−base equilibrium constants
t		time of iradiation
V_R		total volume of the reactor [L]
ζ_i		fraction of the photon rate absorbed by component i (eq 30)
at 172 nm	ζ_{cis}	fraction of the photon rate absorbed by *cis*-cyclooctene
	ζ_{trans}	fraction of the photon rate absorbed by *trans*-cyclooctene
	ζ_{H_2O}	fraction of the photon rate absorbed by H_2O
	ζ_{MeOH}	fraction of the photon rate absorbed by CH_3-OH
$(d[MeOH]/dt)\|_{OH,h\nu}$		total rate of methanol photolysis (reactions 6−9 and 11) yielding hydroxymethyl radicals
$(d[MeOH]/dt)\|h\nu$		total rate of methanol photolysis (reactions 6−9)
$d[MeOH]/dt$		apparent (measured) rate of methanol degradation
$(d[MeOH]/dt)\|_{14}$		rate of methanol production by reaction 14
$d[EG]/dt$		rate of ethylene glycol production
$(d[MeOH]/dt\|_{OH}$		rate of methanol consumption by the reaction with hydroxyl radicals (reaction 11)
$d[HO^\bullet]/dt$		rate of hydroxyl radical production

References and Notes

(1) Eliasson, B.; Kogelschatz, U. *Appl. Phys. B* **1988**, *46*, 299−303.

(2) Stockwald, K. Neuartige Xenon- und Xenon/Quecksilber-Lampen im VUV/ UV-Spektralbereich. Ph.D. Thesis, Universität Karlsruhe (TH), 1991.

(3) We thank R. Kling, and H.-P. Popp, for the spectrophotometric measurements.

(4) Heit, G. Entwicklung und Anwendung neuer Verfahren zur photochemischen Prozessanalyse. Optische In-Situ-Sauerstoffmessung, VUV-Aktinometrie und numerische Simulation. Ph.D. Thesis, Universität Karlsruhe (TH), 1997.

(5) Farhataziz; Rodgers, M. A. J. *Radiation Chemistry*; VCH: Weinheim, 1987, and references cited therein.

(6) Ross, A. B. *Selected specific rates of reactions of transients from water an aqueous solution. Hydrated electron, Supplemental data. National Standard Reference Data System*, National Bureau of Standards; 1975; p 43, Supplement.

(7) Anbar, M.; Farhataziz; Ross, A. B. *Selected specific rates of reactions of transients from water an aqueous solution. II. Hydrogen atom. National Standard Reference Data System*, National Bureau of Standards; 1973, p 51.

(8) Farhataziz; Ross, A. B. *Selected specific rates of reactions of transients from water in aqueous solution. III. Hydroxyl radicals and perhydroxyl radicals and their radical ions. National Standard Reference Data System*, National Bureau of Standards; 1977, p 59.

(9) Bielski, B. H.; Cabelli, D. E.; Arudi, R. L *J. Phys. Chem. Ref. Data* **1985**, *14*, 1041−1100.

(10) von Sonntag, C.; Schuchmann, H.-P. *Angew. Chem.* **1991**, *103*, 1255−1279.

(11) Getoff, N.; Schenck, G. O. *Photochem. Photobiol.* **1968**, *8*, 167−178.

(12) Anbar, M.; Bambenek, M.; Ross, A. B. *Selected specific rates of reactions of transients from water an aqueous solution. 1. Hydrated electron, National Standard Reference Data System*, National Bureau of Standards; 1973, p 43.

(13) Weeks, J. L.; Meaburn, A. C.; Gordon, S. *Radiat. Res.* **1963**, *19*, 559−567.

(14) von Sonntag, C. Photochemistry of saturated alcohols and open-chain ethers at 185 nm in the liquid phase. In McGlynn, S. P., Findley, G. L., Huebner, R. H., Eds.; NATO ASI Series; Photophysics and Photochemistry in the Vaccum Ultraviolet; D. Reidel: Dordrecht, 1985.

(15) Buxton, G. V.; Greenstock, C. L.; Helman, W. P.; Ross, A. B. *J. Phys. Chem. Ref. Data* **1988**, *17*, 513−886.

(16) Spinks, J. W. T.; Woods, R. J. *An Introduction to Radiation Chemistry*; Wiley, New York, 1990.

(17) Asmus, K.-D.; Möckel, H.; Henglein, A. *J. Phys. Chem.* **1973**, *77*, 1218−1221.

(18) Simic, M.; Neta, P.; Hayon, E. *J. Phys. Chem.* **1969**, *73*, 3794−3800.

(19) Adam, W.; Oppenländer, T. *Photochem. Photobiol.* **1984**, *39*, 719−723.

(20) Schuchmann, H.-P.; von Sonntag, C.; Srinivasan, R. *J. Photochem.* **1981**, *15*, 159−162.

(21) Jakob, L.; Kantor, M. M.; Braun, A. M. *J. Inf. Rec. Mater.* **1994**, *21*, 615−616.

(22) Jakob, L. Traitement des eaux par photocatalyse et photolyse V-UV: Degradation oxidative de polluants organiques. Ph.D. Thesis, Ecole Polytechnique Fédérale de Lausanne, 1992.

(23) Hashem, T. M. Ph.D. Thesis, Universität Karlsruhe (TH), 1998.

(24) Heit, G.; Braun, A. M. *Water Sci. Technol.* **1997**, *35*, 25−30.

(25) Heit, G.; Braun, A. M. *J. Inf. Rec.* **1996**, *22*, 543−546.